POLITECNICO DI TORINO
Repository ISTITUZIONALE

Effect of the through-the-thickness temperature distribution on the response of layered and composite shells

(Article begins on next page)

14 May 2024

EFFECT OF THE THROUGH-THE-THICKNESS TEMPERATURE DISTRIBUTION ON THE RESPONSE OF LAYERED AND COMPOSITE SHELLS

SALVATORE BRISCHETTO*

Aeronautics and Space Engineering Department, Politecnico di Torino
corso Duca degli Abruzzi 24, 10129, Torino, Italy

This paper considers the thermal stress problem of thick and thin multilayered cylindrical and spherical shells including carbon fiber reinforced layers and/or a central soft core. The following two cases are considered: - the temperature distribution in thickness direction is assumed linear; - the temperature distribution in thickness direction is calculated via Fourier's heat conduction equation. Carrera's Unified Formulation and the Principle of Virtual Displacements are used to obtain the governing equations in the case of shells with constant radii of curvature subjected to established temperature conditions on their upper and lower surfaces. Both Equivalent Single Layer and Layer Wise models with an order of expansion in the thickness direction from linear to fourth order are considered. The importance of refined models for a correct evaluation of displacement and stress fields in multilayered shells can be noted. Furthermore, it has been shown that results obtained assuming a linear temperature profile in the thickness direction can be meaningless.

Keywords: Composite shells; Fourier's heat conduction equation; refined two-dimensional models; Carrera's Unified Formulation.

1. Introduction

An increasing number of modern aerospace vehicles are made up of composite structures such as multilayered carbon-fiber reinforced and/or sandwich plates and shells. Many of these structures are simultaneously loaded by high thermal and mechanical loads. Typical examples are wings for the next generation of commercial airliners which are exposed to high sun irradiation, large orbital structures under thermal cycling, and the load carrying structure of future reusable launchers. In each of the above mentioned cases, the stress analysis should be preceded by an accurate thermal analysis, which provides the temperature input data required for the stress analysis [Rolfes *et al.*, 1999]. A simplified thermal analysis can be made for thin-walled homogeneous isotropic structures, but it is inappropriate in the case of laminated composite structures.

---

*Aeronautics and Space Engineering Department, Politecnico di Torino, corso Duca degli Abruzzi 24, 10129, Torino, Italy. e.mail: salvatore.brischetto@polito.it

2 *Salvatore Brischetto*

An accurate description of local stress fields in the layers becomes mandatory to prevent thermally loaded structure failure mechanisms [Librescu and Marzocca, 2003a], [Librescu and Marzocca, 2003b]. A satisfactory thermal stress analysis is only possible if: - advanced and refined computational models are developed [Noor and Burton, 1992], [Brischetto and Carrera, 2009]; - correct thermal loads are recognized. For the latter issue, an appropriate temperature profile must be defined (for example by solving Fourier's heat conduction equation) [Carrera, 2002b]: an assumed linear temperature profile is advisable only for thin and homogeneous structures.

Several higher-order two-dimensional models have recently been developed for such problems, which consider only an assumed temperature profile through the thickness. Among these, the higher-order model by Zhen and Wanji [2008], which describes the displacements and stresses in laminated structures in thermal bending, assuming a linear profile of temperature through the thickness z, is of particular interest. The same temperature profile has been used by Khare *et al.* [2003] to obtain a closed-form solution for the thermomechanical analysis of laminated and sandwich shells. Khdeir [1996] and Khdeir *et al.* [1992] have assumed a linear or constant temperature profile through the thickness; the thermoelastic governing equations for laminated shells are exactly solved in the former while a Higher Shear Deformation Theory is given in the latter. An interesting method to analyze the thermal stresses in shells is the use of Cosserat surfaces, as done by Birsan [2009] for two given temperature fields and Iesan [1985] for an assumed polynomial temperature variation in the axial coordinate. Barut *et al.* [2000] analyzed the non-linear thermoelastic behavior of shells by means of the Finite Element Method, but the assigned temperature profile was linear. In the framework of the arbitrary distribution of temperature through the thickness, the work by Miller *et al.* [1981] and Dumir *et al.* [2008] is noteworthy; a classical shell theory for composite shells is given in the former while the importance of the zig-zag form of displacements in the thermal analysis of composite shells is dealt with in the later. In the case of shells, further investigations were made by Hsu *et al.* [1981] for both closed form and Finite Element methods, and by Ding [2008] for a weak formulation for the case of state equations, including boundary conditions. The importance of mechanical and thermal anisotropy in such investigations was remarked on by Padovan [1976]. Some interesting experimental results can be found in Holstein *et al.* [1998]; Kapuria *et al.* [1997] have suggested the use of piezoelectric layers to contrast such thermal deformations. Librescu and Lin [1999] have suggested the use of linear temperature profile to investigate the importance of refined kinematics in the case of multilayered composite shells, which has also been dealt with in a companion paper by Brischetto and Carrera [2009]. The importance of refined kinematic models is well-known [Brischetto and Carrera, 2009]. The present paper investigates the importance of the temperature profile in the thermal stress analysis of composite shells, as already done by Carrera [2002b] and Carrera [2000] for the case of

multilayered plates.

In literature, several works underline the importance of a calculated temperature profile. Some of these are listed in the following. A Finite Element shell has been developed by Rolfes *et al.* [1999] to analyze the composite structures simultaneously loaded by mechanical and thermal loads; the temperature profile is presumed linear or quadratic in the thickness direction and then introduced into Fourier's law of heat conduction. The same procedure for the temperature profile has been repeated by Rolfes and Rohwer [2000] in the case of 2D finite elements for composite plates and shells. In order to investigate the effects of interfacial imperfections on laminated composite shells under thermal loads, Cheng and Batra [2001] have made a comparison between a constant through the thickness distribution of temperature and the temperature field through the thickness obtained by solving the heat conduction equation. Other important cases in which the calculated temperature profile is mandatory are the functionally graded material (FGM) structures, and the cases of coupling between the thermal field and other physical fields, such as the electrical one. Pellitier and Vel [2006] have given a three-dimensional solution for functionally graded cylindrical shells subjected to thermal and mechanical loads. A semi-inverse method for the heat conduction problem was employed to obtain a second-order differential equation that is solved assuming a solution in the form of a power series. Santos *et al.* [2008] have used a two-dimensional model for the thermoelastic analysis of cylindrical shells subjected to transient thermal shock loading; the temperature profile has obtained writing Fourier's heat conduction equation for the heat transfer in cylindrical coordinates. In the case of postbuckling of FGM cylindrical shells under mechanical loading in thermal environments, Shen and Noda [2005] have obtained the temperature along the thickness, solving a steady-state heat transfer equation. The same equation has been solved by Shen [2005] in order to obtain the temperature distribution when the shell is subjected to electric loads in thermal environments. The importance of the thickness ratio has been underlined by Vel and Pelletier [2007]; for thick structures, there is in fact a substantial difference between a prescribed temperature load and an applied heat flux, if Fourier's law of heat conduction is considered. Wu *et al.* [2005] have investigated the thermal buckling of FGM shells subjected to thermal load. Closed form solutions were provided for three types of thermal load: - uniform temperature rise, when the temperature changes uniformly through the thickness; - linear temperature change, when the temperature change is linear through the thickness; - non-linear temperature change, when the temperature rises differently at the inner and outer surfaces of the shell and the temperature distribution across the thickness is governed by the steady state heat conduction equation and boundary conditions. A very interesting application could be the postbuckling analysis of functionally graded shells with piezoelectric actuators subjected to hydrostatic pressure combined with electric loads in thermal environments as shown by Shen and Noda [2007]. The temperature variation only occurs in the thickness direction and a one dimensional temperature field is assumed

4   *Salvatore Brischetto*

to be constant in the $\alpha\beta$ plane of the shell. In such a case, the temperature distribution along the thickness can be obtained by solving a steady-state heat transfer equation.

The employed kinematic models are described in Section 2 and details can be found in the overview of Carrera's Unified Formulation (CUF) [Carrera, 1995], [Carrera, 2002a]. Equivalent Single Layer and Layer Wise models have been obtained referring to the Principle of Virtual Displacements (PVD). Section 3 discusses the temperature profile. It can be assumed linear, as already shown in [Brischetto and Carrera, 2009], or it can be calculated by solving the heat conduction Fourier's equation, as already illustrated in [Carrera, 2002b] and [Brischetto *et al.*, 2008]. Section 4 describes how the general governing equations and their closed form can be obtained (for details reference can be made to Brischetto and Carrera [2009]). The results and discussion are reported in Section 5. Section 6 gives the main conclusions.

2. Carrera's Unified Formulation

Carrera's Unified Formulation (CUF) [Carrera, 1995] permits a large variety of two-dimensional models to be obtained in the case of bi-dimensional multi-layered structures such as plates and shells. In this section, CUF is described for shells of constant thickness h and radii of curvature R_α and R_β. The geometry and reference system are shown in Fig. 1. The displacement components u_α, u_β and u_z are measured with respect to the α, β and z axes. The latter axis denotes the through-the-thickness direction. Ω is the shell/plate reference surface. In the case of plates, the curvilinear coordinates α and β coincide with the Cartesian ones x and y, where u_x, u_y and u_z are the displacement components.

The obtained hierarchical models differ in the order of used expansion in the thickness direction and in the manner the variables are modelled (Equivalent Single Layer (ESL) or Layer Wise (LW) approach). The salient feature of CUF is the unified manner in which all the considered variables and fields (displacement and temperature) can be treated. The considered variables and their variations are split into a set of thickness functions and the relative terms only depend on in-plane coordinates (α,β). According to this separation, a general variable $\boldsymbol{a}$ and its respective variation $\delta\boldsymbol{a}$ can be written as:

$$\boldsymbol{a}(\alpha,\beta,z) = F_\tau(z)\,\boldsymbol{a}_\tau(\alpha,\beta), \quad \delta\boldsymbol{a}(\alpha,\beta,z) = F_s(z)\,\delta\boldsymbol{a}_s(\alpha,\beta), \quad \tau,s = 1,\ldots,N\,, \ (1)$$

where N is the order of expansion in the thickness direction.

2.1. *Equivalent Single Layer theories*

Equivalent Single Layer models are based on the assumption of a global description of the displacement field along the whole shell thickness; a Taylor expansion is used:

$$\boldsymbol{u}(\alpha,\beta,z) = F_\tau(z)\boldsymbol{u}_\tau(\alpha,\beta) = z^r\boldsymbol{u}_r(\alpha,\beta)\,, \qquad r = 0,1,2,\ldots,N\,, \qquad (2)$$
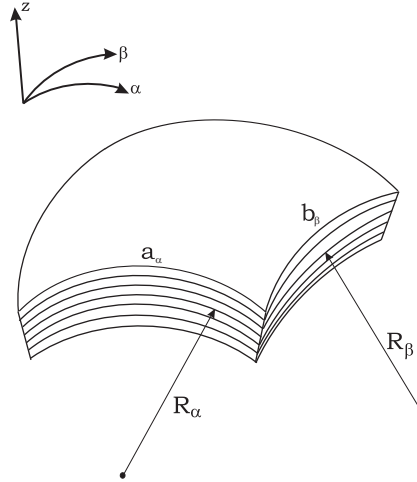
Fig. 1.   Geometry and notations for a cylindrical shell.

where the displacement vector is $\boldsymbol{u} = (u_\alpha, u_\beta, u_z)$.

The summing convention for the repeated indexes has been adopted. N is the order of expansion, which is taken as a free parameter. In the numerical investigation N is considered to be as low as 1 and as high as 4. According to the acronym system developed within CUF, the related theories are named as ED1-ED4. The letter E denotes that the kinematic is preserved for the whole layers, as in the ESL approach. D denotes that only displacement unknowns are used and the last number states the through-the-thickness expansion order.

Classical models such as the First order Shear Deformation Theory (FSDT) and the Classical Lamination Theory (CLT) are obtained from ED1 by imposing a constant through the thickness transverse displacement, and considering an infinite shear factor for the CLT. In case of models with constant or linear transverse displacement (CLT, FSDT and ED1), the plane-stress conditions are imposed as illustrated in Carrera and Brischetto [2008a] and Carrera and Brischetto [2008b] to avoid the Poisson's locking phenomena.

2.2. *Layer Wise theories*

Multilayered plates and shells can be analyzed by kinematic assumptions which are independent in each layer. According to Reddy [2004] these approaches are herein stated as Layer-Wise (LW) theories.

LW description yields, thus, displacement variables that are independent in each layer. The Taylor's thickness expansion, adopted in the previous paragraph for ESL cases, is not convenient for LW description. Displacements interlaminar continuity can be imposed more conveniently by employing interface values as unknown

6   *Salvatore Brischetto*

variables. LW description assumes the following form:

$$
\boldsymbol{u}^k(\alpha, \beta, z) = F_t(z)\, \boldsymbol{u}_t^k(\alpha, \beta) + F_b(z)\boldsymbol{u}_b^k(\alpha, \beta) + F_r(z)\boldsymbol{u}_r^k(\alpha, \beta)\ ,
$$
$$
r = 2, 3, .., N\ ,\ \ k = 1, 2, .., N_l\ .
\tag{3}
$$

N_l indicates the number of layers. Subscripts t and b denote values related to the top and the bottom of each layer, respectively. The thickness functions $F_\tau(\zeta_k)$ have been defined by:

$$
F_t = \tfrac{P_0 + P_1}{2}\ ,\quad F_b = \tfrac{P_0 - P_1}{2}\ ,\quad F_r = P_r - P_{r-2}\ ,\qquad r = 2, 3, .., N\ ,
\tag{4}
$$

in which $P_j = P_j(\zeta_k)$ is the Legendre's j^{th}-order polynomial defined in the ζ_k- domain : $-1 \le \zeta_k \le 1$. In numerical investigations the maximum considered order of expansion is four, related polynomials are:

$$
P_0 = 1\ ,\ \ P_1 = \zeta_k\ ,\ \ P_2 = \frac{(3\zeta_k^2 - 1)}{2}\ ,\ \ P_3 = \frac{5\zeta_k^3 - 3\zeta_k}{2}\ ,\ \ P_4 = \frac{35\zeta_k^4}{8} - \frac{15\zeta_k^2}{4} + \frac{3}{8}\ .
$$

The previous functions have the following interesting properties:

$$
\zeta_k = \begin{cases} 1 : F_t = 1; F_b = 0; F_r = 0 \\ -1 : F_t = 0; F_b = 1; F_r = 0\ . \end{cases}
\tag{5}
$$

The top and bottom values have been used as unknown variables. The interlaminar compatibility of displacement can be therefore easily linked (see Fig. 2):

$$
\boldsymbol{u}_t^k = \boldsymbol{u}_b^{(k+1)}\ ,\quad k = 1, N_l - 1\ .
\tag{6}
$$

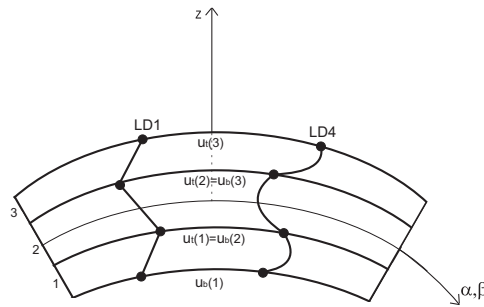The acronyms for these theories are LD1-LD4, with L that means Layer Wise approach.

Fig. 2.   Displacement in Layer Wise form through the thickness of a multilayered shell.

3. Temperature profile

If the values of the temperature are known at the top and bottom surface of the plate, the temperature profile through the thickness can be considered in two different ways. The first method introduces an assumed profile $T(z)$ that varies linearly from the top to the bottom; the second one computes $T(z)$ by solving Fourier's heat conduction equation. The temperature is assumed bi-sinusoidal in the plane (α, β) at the top and bottom shell surfaces:

$$T(\alpha, \beta, z) = \hat{T}(z) \sin(\frac{m\pi}{a_\alpha}\alpha) \sin(\frac{n\pi}{b_\beta}\beta) , \qquad (7)$$

with amplitudes $\hat{T}(+h/2) = T_t = +0.5$ and $\hat{T}(-h/2) = T_b = -0.5$. a_α and b_β are the shell dimensions. m and n are the waves number. In the case of assumed temperature profile (T_a) a linear through the thickness distribution is considered from $+0.5$ to -0.5. Independently by the number of considered layers the linear profile is always the same as indicated in Fig. 3. The temperature profile is approximated as displacements in case of the Layer Wise approach:

$$T^k(\alpha, \beta, z) = F_\tau \, \theta_\tau^k \qquad \text{with} \quad \tau = t, b, r \quad \text{and} \quad r = 2, \ldots, 4 , \qquad (8)$$

t and b indicate the top and bottom of the considered k^{th} layer. The thickness functions F_τ are a combination of Legendre's polynomials.

If the temperature is assumed linear through the thickness, the values at the top and bottom surface, and therefore F_t and F_b, would be sufficient to describe the assumed profile via CUF.

The calculation procedure for the actual temperature in case of one or more layers is reported in the following in order to obtain the values of θ_τ^k for Eq.(8).

If the considered shell is subjected to a bi-sinusoidal thermal load at the top and the bottom, the thermal boundary conditions are:

$$T = 0 \qquad \text{at} \quad \alpha = 0, a_\alpha \quad \text{and} \quad \beta = 0, b_\beta$$

$$T = T_b \, \sin\left(\frac{m\pi\alpha}{a_\alpha}\right) \, \sin\left(\frac{n\pi\beta}{b_\beta}\right) \qquad \text{at} \quad z = -\frac{h}{2} \quad \text{with} \quad b : \text{bottom}$$

$$T = T_t \, \sin\left(\frac{m\pi\alpha}{a_\alpha}\right) \, \sin\left(\frac{n\pi\beta}{b_\beta}\right) \qquad \text{at} \quad z = +\frac{h}{2} \quad \text{with} \quad t : \text{top} , \qquad (9)$$

where m and n are the waves number along the two in-plane shell directions (α, β). a_α and b_β are the shell dimensions, h is the shell thickness, and T_b and T_t are the amplitudes of the temperature at the bottom and top, respectively.

In case of multi-layered structures, continuity conditions for the temperature T and the transverse normal heat flux q_z hold in the thickness direction at each kth layer interface, reading:

$$T_t^k = T_b^{k+1} , \qquad q_{z\,t}^k = q_{z\,b}^{k+1} \qquad \text{for} \quad k = 1, \ldots, N_l - 1 , \qquad (10)$$

where N_l is the number of layers in the considered structure.

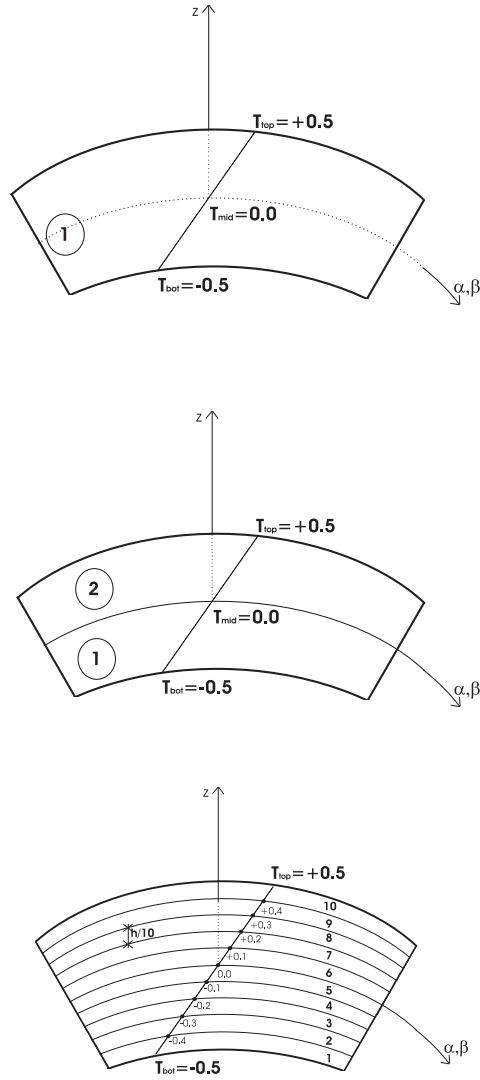8   *Salvatore Brischetto*

Fig. 3.   Linear assumed profile of temperature through the thickness of the one-layered, two-layered and ten-layered cylindrical shell.

The relationship between the transverse heat flux and the temperature is given as:

$$q_z^k = K_3^k \, \frac{\partial T^k}{\partial z} \ . \tag{11}$$

In general for the kth homogeneous orthotropic layer, the differential Fourier's equa-

tion of heat conduction reads:

$$\left(\frac{K_1^k}{H_\alpha^2}\right) \frac{\partial^2 T}{\partial \alpha^2} + \left(\frac{K_2^k}{H_\beta^2}\right) \frac{\partial^2 T}{\partial \beta^2} + K_3^k \frac{\partial^2 T}{\partial z^2} = 0 \; . \tag{12}$$

K_1^k, K_2^k and K_3^k are the thermal conductivities along the three shell directions α, β and z, that are constant in each layer. ∂ indicates the partial derivative. $H_\alpha = (1 + z^k/R_\alpha^k)$ and $H_\beta = (1 + z^k/R_\beta^k)$ are the metric coefficients (for details see Section 4.1). In case of plates Eq.(12) can be easily solved because $H_\alpha = H_\beta = 1$ and the coefficients K_1^k, K_2^k and K_3^k are constant for each layer k. In case of shell we can define three new coefficients $K_1^{*k} = \frac{K_1^k}{H_\alpha^2}$, $K_2^{*k} = \frac{K_2^k}{H_\beta^2}$ and $K_3^{*k} = K_3^k$, which in a generic layer k depend on the thickness coordinate of the shell, so:

$$K_1^{*k} \frac{\partial^2 T}{\partial \alpha^2} + K_2^{*k} \frac{\partial^2 T}{\partial \beta^2} + K_3^{*k} \frac{\partial^2 T}{\partial z^2} = 0 \; . \tag{13}$$

Eq.(13) has not constant coefficients in the layer k. It can be solved by introducing for each layer k a given number of mathematical layers (N_{ml}). Considering with N_l the number of physical layers, a new index j can be defined which goes from 1 to $(N_l \times N_{ml})$. So the continuity of temperature and transverse heat flux can be written in each jth mathematical interface:

$$T_t^j = T_b^{j+1} \; , \qquad q_{z\,t}^j = q_{z\,b}^{j+1} \qquad \text{for} \quad j = 1, \ldots, (N_l \times N_{ml} - 1) \; , \tag{14}$$

where

$$q_z^j = K_3^j \frac{\partial T^j}{\partial z} \; . \tag{15}$$

Eq.(13) can be rewritten for each mathematical layer j:

$$K_1^{*j} \frac{\partial^2 T}{\partial \alpha^2} + K_2^{*j} \frac{\partial^2 T}{\partial \beta^2} + K_3^{*j} \frac{\partial^2 T}{\partial z^2} = 0 \; . \tag{16}$$

In these mathematical layers we can suppose K_1^{*j} and K_2^{*j} constant because in each mathematical layer we can calculate the values of H_α and H_β.

For a mathematical layer, both governing equations and boundary conditions are satisfied by assuming the following temperature field:

$$T(\alpha, \beta, z) = f(z) \, \sin\left(\frac{m\pi\alpha}{a_\alpha}\right) \, \sin\left(\frac{n\pi\beta}{b_\beta}\right) \tag{17}$$

with

$$f(z) = T_0 \, \exp\left(s^j \, z\right) \; , \tag{18}$$

T_0 is a constant and s^j a parameter. Substituting Eq.(17) in Eq.(16) and solving for s^j:

$$s_{1,2}^j = \pm \sqrt{\frac{K_1^{*j} \left(\frac{m\pi}{a_\alpha}\right)^2 + K_2^{*j} \left(\frac{n\pi}{b_\beta}\right)^2}{K_3^{*j}}} \; . \tag{19}$$

Therefore:

$$f(z) = T_{01}^j \ \exp\left(s_1^j \, z\right) + T_{02}^j \ \exp\left(s_1^j \, z\right) \ \ \text{or} \ \ f(z) = C_1^j \ \cosh\left(s_1^j \, z\right) + C_2^j \ \sinh\left(s_1^j \, z\right) \ . \tag{20}$$

The solution for a mathematical layer j can be written as:

$$T_c(\alpha, \beta, z) = T^j = \left[C_1^j \cosh\left(s_1^j z\right) + C_2^j \sinh\left(s_1^j z\right)\right] \ \sin\left(\frac{m\pi\alpha}{a_\alpha}\right) \sin\left(\frac{n\pi\beta}{b_\beta}\right) \ , \tag{21}$$

wherein the coefficients C_1^j and C_2^j are constant for each mathematical layer j.

In Eq.(20) for each mathematical layer j two unknowns (C_1^j and C_2^j) remain. Therefore, if the number of layers is N_l, the number of mathematical layers are $N_l \times N_{ml}$, the number of unknowns is $2N_l \times N_{ml}$ and we need $2N_l \times N_{ml}$ equations to determine the unknowns.

As we know the temperature at the top and the bottom surface, we have already two conditions:

$$T_{bot} = C_1^1 \ \cosh\left(s_1^1 z_{bot}\right) + C_2^1 \ \sinh\left(s_1^1 z_{bot}\right) \ ,$$

$$T_{top} = C_1^{N_l \times N_{ml}} \ \cosh\left(s_1^{N_l \times N_{ml}} z_{top}\right) + C_2^{N_l \times N_{ml}} \ \sinh\left(s_1^{N_l \times N_{ml}} z_{top}\right) \ . \tag{22}$$

Another $(N_l \times N_{ml} - 1)$ equations can be obtained from the continuity of temperature at each mathematical interface, and finally $(N_l \times N_{ml} - 1)$ equations result from the continuity of the heat flux through the interfaces, compare Eq.(14). Thus, we have:

$$C_1^j \ \cosh\left(s_1^j z_t^j\right) + C_2^j \ \sinh\left(s_1^j z_t^j\right) - C_1^{j+1} \ \cosh\left(s_1^{j+1} z_b^{j+1}\right)$$

$$- C_2^{j+1} \ \sinh\left(s_1^{j+1} z_b^{j+1}\right) = 0 \ ,$$

$$s_1^j \ K_3^j \left[C_1^j \ \cosh(s_1^j z_t^j) + C_2^j \ \sinh(s_1^j z_t^j)\right]$$

$$- s_1^{j+1} \ K_3^{j+1} \left[C_1^{j+1} \ \cosh\left(s_1^{j+1} z_b^{j+1}\right) - C_2^{j+1} \ \sinh\left(s_1^{j+1} z_b^{j+1}\right)\right] = 0 \ . \tag{23}$$

In Eqs.(22) and (23), z_{top} and z_{bot} indicate the coordinates of top and bottom of the whole shell. z_t^j and z_b^{j+1} represent the top of the jth mathematical layer and the bottom of the $(j + 1)^{th}$ mathematical layer, respectively.

Solving the system given by Eqs.(22) and (23), we gain the $2N_l \times N_{ml}$ coefficients C_1^j and C_2^j. The actual temperature amplitude in the thickness shell direction is then given by:

$$T_c(z) = T^j = C_1^j \ \cosh\left(s_1^j z\right) + C_2^j \ \sinh\left(s_1^j z\right) \quad \text{with} \quad j = 1, \ldots, (N_l \times N_{ml}) \ . \tag{24}$$

We compute the temperature at different values z_N of the thickness coordinate. By

solving the system in Eq.(25), we obtain the N values of θ_τ^k for the CUF:

$$
\begin{bmatrix}
T_c(z_1) \\
T_c(z_2) \\
\vdots \\
T_c(z_N)
\end{bmatrix}
=
\begin{bmatrix}
F_0(z_1) & F_1(z_1) & \cdots & F_N(z_1) \\
F_0(z_2) & F_1(z_2) & \cdots & F_N(z_2) \\
\vdots & \vdots & \vdots & \vdots \\
F_0(z_N) & F_1(z_N) & \cdots & F_N(z_N)
\end{bmatrix}
\begin{bmatrix}
\theta_0^k \\
\theta_1^k \\
\vdots \\
\vdots \\
\theta_N^k
\end{bmatrix} .
\tag{25}
$$

So, if we consider a generic multilayered shell, the temperature profile is approximated by Eq.(8) and the N values of θ_τ^k are given by Eq.(25). In Eq.(25) T_c is calculated by means of the mathematical layers j in certain points that permit the correspondence with the physical layers k.

4. Governing equations

In order to obtain the governing equations for the thermo-mechanical analysis of multilayered shells, the Principle of Virtual Displacements is employed. The used geometrical and constitutive relations are discussed in the following.

4.1. *Geometrical relations*

Shells and plates are bi-dimensional structures where one dimension, in general the thickness in z direction, is neglected respect to the others two in the plane. Shells have curvature along the in-plane directions, in this paper only shells with constant radii of curvature are considered. The geometry and reference system for shells are indicated in Fig. 1.

For a shell, the square of an infinitesimal linear segment in the layer, the associated infinitesimal area and volume elements are given by:

$$
ds_k^2 = H_\alpha^{k\,2}\, d\alpha_k^2 \; + \; H_\beta^{k\,2}\, d\beta_k^2 + H_z^{k\,2}\, dz_k^2 \; ,
$$

$$
d\Omega_k = H_\alpha^k H_\beta^k\, d\alpha_k\, d\beta_k \; ,
$$

$$
dV_k = H_\alpha^k\, H_\beta^k\, H_z^k\, d\alpha_k\, d\beta_k\, dz_k \; ,
\tag{26}
$$

where the metric coefficients are:

$$
H_\alpha^k = A^k(1 + z_k/R_\alpha^k), \quad H_\beta^k = B^k(1 + z_k/R_\beta^k), \quad H_z^k = 1 \; .
\tag{27}
$$

k denotes the kth layer of the multilayered shell; R_α^k and R_β^k are the principal radii of curvature along the coordinates α_k and β_k, respectively. A^k and B^k are the coefficients of the first fundamental form of Ω_k (Γ_k is the Ω_k boundary) [Leissa, 1973]. In this paper, the attention has been restricted to shells with constant radii of curvature, so $A^k = B^k = 1.0$.

12   *Salvatore Brischetto*

Given a kth layer, geometrical relations permit to express in-plane $\boldsymbol{\epsilon_p}$ and out-of-plane $\boldsymbol{\epsilon_n}$ strains in terms of displacement $\boldsymbol{u}$. The following relations hold in the case of a shell:

$$\boldsymbol{\epsilon}_{pG} = [\epsilon_{\alpha\alpha}, \epsilon_{\beta\beta}, \epsilon_{\alpha\beta}]^T = (\boldsymbol{D}_p + \boldsymbol{A}_p)\,\boldsymbol{u}\ ,$$
$$\boldsymbol{\epsilon}_{nG} = [\epsilon_{\alpha z}, \epsilon_{\beta z}, \epsilon_{zz}]^T = (\boldsymbol{D}_{np} + \boldsymbol{D}_{nz} - \boldsymbol{A}_n)\,\boldsymbol{u} \tag{28}$$

where $\boldsymbol{u} = (u_\alpha, u_\beta, u_z)$. The explicit form of introduced arrays follows:

$$\boldsymbol{D}_p = \begin{bmatrix} \frac{\partial_\alpha}{H_\alpha} & 0 & 0 \\ 0 & \frac{\partial_\beta}{H_\beta} & 0 \\ \frac{\partial_\beta}{H_\beta} & \frac{\partial_\alpha}{H_\alpha} & 0 \end{bmatrix}\ , \quad \boldsymbol{D}_{np} = \begin{bmatrix} 0 & 0 & \frac{\partial_\alpha}{H_\alpha} \\ 0 & 0 & \frac{\partial_\beta}{H_\beta} \\ 0 & 0 & 0 \end{bmatrix}\ , \quad \boldsymbol{D}_{nz} = \begin{bmatrix} \partial_z & 0 & 0 \\ 0 & \partial_z & 0 \\ 0 & 0 & \partial_z \end{bmatrix}\ ,$$

$$\boldsymbol{A}_p = \begin{bmatrix} 0 & 0 & \frac{1}{H_\alpha R_\alpha} \\ 0 & 0 & \frac{1}{H_\beta R_\beta} \\ 0 & 0 & 0 \end{bmatrix}\ , \quad \boldsymbol{A}_n = \begin{bmatrix} \frac{1}{H_\alpha R_\alpha} & 0 & 0 \\ 0 & \frac{1}{H_\beta R_\beta} & 0 \\ 0 & 0 & 0 \end{bmatrix}\ . \tag{29}$$

4.2. *Constitutive relations*

Stresses for thermomechanical problems have two parts, a mechanical part denoted with the subscript d and a thermal one denoted with the subscript t. In order to use the Principle of Virtual Displacements (PVD), the stresses are split in in-plane components $\boldsymbol{\sigma}_p = (\sigma_{\alpha\alpha}, \sigma_{\beta\beta}, \sigma_{\alpha\beta})$ and in out-of-plane ones $\boldsymbol{\sigma}_n = (\sigma_{\alpha z}, \sigma_{\beta z}, \sigma_{zz})$.

The constitutive equations are given as:

$$\boldsymbol{\sigma}_{pC}^k = \boldsymbol{\sigma}_{pd}^k - \boldsymbol{\sigma}_{pt}^k = \boldsymbol{C}_{pp}^k\,\boldsymbol{\epsilon}_{pG}^k + \boldsymbol{C}_{pn}^k\,\boldsymbol{\epsilon}_{nG}^k - \boldsymbol{\lambda}_p^k\,T^k\ ,$$
$$\boldsymbol{\sigma}_{nC}^k = \boldsymbol{\sigma}_{nd}^k - \boldsymbol{\sigma}_{nt}^k = \boldsymbol{C}_{np}^k\,\boldsymbol{\epsilon}_{pG}^k + \boldsymbol{C}_{nn}^k\,\boldsymbol{\epsilon}_{nG}^k - \boldsymbol{\lambda}_n^k\,T^k\ , \tag{30}$$

where subscript C indicates the constitutive equations and G the geometrical ones. The coefficients $\boldsymbol{\lambda}_p^k$ and $\boldsymbol{\lambda}_n^k$ are linked to the coefficients of thermal expansion $\boldsymbol{\alpha}_p^k$ and $\boldsymbol{\alpha}_n^k$ by:

$$\boldsymbol{\lambda}_p^k = \boldsymbol{\lambda}_{pp}^k + \boldsymbol{\lambda}_{pn}^k = \boldsymbol{C}_{pp}^k\,\boldsymbol{\alpha}_p^k + \boldsymbol{C}_{pn}^k\,\boldsymbol{\alpha}_n^k\ ,$$
$$\boldsymbol{\lambda}_n^k = \boldsymbol{\lambda}_{np}^k + \boldsymbol{\lambda}_{nn}^k = \boldsymbol{C}_{np}^k\,\boldsymbol{\alpha}_p^k + \boldsymbol{C}_{nn}^k\,\boldsymbol{\alpha}_n^k\ , \tag{31}$$

with the elastic coefficients allocated in the following four sub-arrays:

$$\boldsymbol{C}_{pp}^k = \begin{bmatrix} C_{11}^k & C_{12}^k & C_{16}^k \\ C_{12}^k & C_{22}^k & C_{26}^k \\ C_{16}^k & C_{26}^k & C_{66}^k \end{bmatrix}\ , \qquad \boldsymbol{C}_{pn}^k = \begin{bmatrix} 0 & 0 & C_{13}^k \\ 0 & 0 & C_{23}^k \\ 0 & 0 & C_{36}^k \end{bmatrix}\ ,$$

$$\boldsymbol{C}_{np}^k = \begin{bmatrix} 0 & 0 & 0 \\ 0 & 0 & 0 \\ C_{13}^k & C_{23}^k & C_{36}^k \end{bmatrix}\ , \qquad \boldsymbol{C}_{nn}^k = \begin{bmatrix} C_{55}^k & C_{45}^k & 0 \\ C_{45}^k & C_{44}^k & 0 \\ 0 & 0 & C_{33}^k \end{bmatrix}\ . \tag{32}$$

The thermal expansion coefficients and the coefficients of thermo-mechanical coupling are:

$$
\boldsymbol{\alpha}_p^k = \begin{bmatrix} \alpha_{11}^k \\ \alpha_{22}^k \\ 0 \end{bmatrix} , \ \boldsymbol{\alpha}_n^k = \begin{bmatrix} 0 \\ 0 \\ \alpha_{33}^k \end{bmatrix} , \ \boldsymbol{\lambda}_{pp}^k = \begin{bmatrix} \lambda_{pp1}^k \\ \lambda_{pp2}^k \\ \lambda_{pp3}^k \end{bmatrix} , \ \boldsymbol{\lambda}_{pn}^k = \begin{bmatrix} \lambda_{pn1}^k \\ \lambda_{pn2}^k \\ \lambda_{pn3}^k \end{bmatrix} ,
$$

$$
\boldsymbol{\lambda}_{np}^k = \begin{bmatrix} 0 \\ 0 \\ \lambda_{np3}^k \end{bmatrix} , \ \boldsymbol{\lambda}_{nn}^k = \begin{bmatrix} 0 \\ 0 \\ \lambda_{nn3}^k \end{bmatrix} . \tag{33}
$$

4.3. *Fundamental nuclei*

This section presents the derivation of governing equations based on the *Principle of Virtual Displacements* (PVD) in case of a multilayered shell subjected to thermal and/or mechanical loads. A closed form solution will be developed considering particular materials and boundary conditions. The procedure permits to obtain the so-called *fundamental nuclei* which are simple matrices representing the basic elements from which the stiffness matrices of the whole structure can be computed.

We consider a multi-layered shell with N_l layers. The PVD for the thermomechanical case reads:

$$
\sum_{k=1}^{N_l} \int_{\Omega_k} \int_{A_k} \left\{ \delta \boldsymbol{\epsilon}_{pG}^k{}^T \boldsymbol{\sigma}_{pC}^k + \delta \boldsymbol{\epsilon}_{nG}^k{}^T \boldsymbol{\sigma}_{nC}^k \right\} d\Omega_k dz = \sum_{k=1}^{N_l} \delta L_e^k \ , \tag{34}
$$

where Ω_k and A_k are the integration domains in plane (α, β) and z directions, respectively. k indicates the layer and T the transpose of a vector. δL_e^k is the external work for the kth layer. G means geometrical relations and C constitutive ones. $\boldsymbol{\sigma}_{pC}^k$ and $\boldsymbol{\sigma}_{nC}^k$ contain the mechanical (d) and thermal (t) contributions, so:

$$
\sum_{k=1}^{N_l} \int_{\Omega_k} \int_{A_k} \left\{ \delta \boldsymbol{\epsilon}_{pG}^k{}^T (\boldsymbol{\sigma}_{pd}^k - \boldsymbol{\sigma}_{pt}^k) + \delta \boldsymbol{\epsilon}_{nG}^k{}^T (\boldsymbol{\sigma}_{nd}^k - \boldsymbol{\sigma}_{nt}^k) \right\} d\Omega_k dz = \sum_{k=1}^{N_l} \delta L_e^k \ . \tag{35}
$$

The steps to obtain the governing equations are:

- substitution of geometrical relations (subscript G),
- substitution of appropriate constitutive equations (subscript C),
- introduction of the CUF (see Section 2).

The complete procedure to obtain the governing equations and the fundamental nuclei are reported in a previous author's work [Brischetto and Carrera, 2009]. Here, the governing equations are reported in general form for a multilayered shell subjected to thermal and mechanical loadings:

$$
\delta \boldsymbol{u}_s^k{}^T : \qquad \boldsymbol{K}_{uu}^{k\tau s} \, \boldsymbol{u}_\tau^k = -\boldsymbol{K}_{u\theta}^{k\tau s} \, \boldsymbol{\theta}_\tau^k \, + \, \boldsymbol{P}_{u\tau}^k \tag{36}
$$

14   *Salvatore Brischetto*

with related boundary conditions on edge Γ_k:

$$\boldsymbol{\Pi}_d^{k\tau s}\,\boldsymbol{u}_\tau^k \,-\, \boldsymbol{\Pi}_t^{k\tau s}\,\theta_\tau^k \,=\, \boldsymbol{\Pi}_d^{k\tau s}\,\bar{\boldsymbol{u}}_\tau^k \,-\, \boldsymbol{\Pi}_t^{k\tau s}\,\bar{\theta}_\tau^k \,, \tag{37}$$

where $(-\boldsymbol{K}_{u\theta}^{k\tau s}\boldsymbol{\theta}_\tau^k)$ is the thermal load and $\boldsymbol{P}_{u\tau}^k$ is the external mechanical one. The fundamental nuclei $\boldsymbol{K}_{uu}^{k\tau s}$ and $\boldsymbol{K}_{u\theta}^{k\tau s}$ have to be assembled by expanding the indices as described in the following: via τ and s we consider the expansion in z for the considered variables, and via k the assembling on the number of layers is accomplished.

Considering the Eqs.(26), the fundamental nuclei are:

$$\boldsymbol{K}_{uu}^{k\tau s} = \int\limits_{A_k} \Big[\Big(-\boldsymbol{D}_p^k + \boldsymbol{A}_p^k \Big)^T \Big(\boldsymbol{C}_{pp}^k (\boldsymbol{D}_p^k + \boldsymbol{A}_p^k) \,+\, \boldsymbol{C}_{pn}^k (\boldsymbol{D}_{np}^k + \boldsymbol{D}_{nz}^k - \boldsymbol{A}_n^k) \Big) +$$

$$\Big(-\boldsymbol{D}_{np}^k + \boldsymbol{D}_{nz}^k - \boldsymbol{A}_n^k \Big)^T \Big(\boldsymbol{C}_{np}^k (\boldsymbol{D}_p^k + \boldsymbol{A}_p^k) +$$

$$\boldsymbol{C}_{nn}^k (\boldsymbol{D}_{np}^k + \boldsymbol{D}_{nz}^k - \boldsymbol{A}_n^k) \Big) \Big] F_s F_\tau H_\alpha^k H_\beta^k dz \,, \tag{38}$$

$$\boldsymbol{K}_{u\theta}^{k\tau s} = \int\limits_{A_k} \Big[\Big(-\boldsymbol{D}_p^k + \boldsymbol{A}_p^k \Big)^T \Big(-\boldsymbol{\lambda}_p^k \Big) + \Big(-\boldsymbol{D}_{np}^k + \boldsymbol{D}_{nz}^k - \boldsymbol{A}_n^k \Big)^T$$

$$\Big(-\boldsymbol{\lambda}_n^k \Big) \Big] F_s F_\tau H_\alpha^k H_\beta^k dz \,, \tag{39}$$

$$\boldsymbol{\Pi}_d^{k\tau s} = \int\limits_{A_k} \Big[\boldsymbol{I}_p^{kT} \Big(\boldsymbol{C}_{pp}^k (\boldsymbol{D}_p^k + \boldsymbol{A}_p^k) \,+\, \boldsymbol{C}_{pn}^k (\boldsymbol{D}_{np}^k + \boldsymbol{D}_{nz}^k - \boldsymbol{A}_n^k) \Big) +$$

$$\boldsymbol{I}_{np}^{kT} \Big(\boldsymbol{C}_{np}^k (\boldsymbol{D}_p^k + \boldsymbol{A}_p^k) \,+\, \boldsymbol{C}_{nn}^k (\boldsymbol{D}_{np}^k + \boldsymbol{D}_{nz}^k - \boldsymbol{A}_n^k) \Big) \Big] F_s F_\tau H_\alpha^k H_\beta^k dz \,, \tag{40}$$

$$\boldsymbol{\Pi}_t^{k\tau s} = \int\limits_{A_k} \Big[\boldsymbol{I}_p^{kT} \Big(-\boldsymbol{\lambda}_p^k \Big) + \boldsymbol{I}_{np}^{kT} \Big(-\boldsymbol{\lambda}_n^k \Big) \Big] F_s F_\tau H_\alpha^k H_\beta^k dz \,, \tag{41}$$

with

$$\boldsymbol{I}_p^k = \begin{bmatrix} \frac{1}{H_\alpha^k} & 0 & 0 \\ 0 & \frac{1}{H_\beta^k} & 0 \\ \frac{1}{H_\beta^k} & \frac{1}{H_\alpha^k} & 0 \end{bmatrix} \,, \quad \boldsymbol{I}_{np}^k = \begin{bmatrix} 0 & 0 & \frac{1}{H_\alpha^k} \\ 0 & 0 & \frac{1}{H_\beta^k} \\ 0 & 0 & 0 \end{bmatrix} \,. \tag{42}$$

4.4. *Closed form solution*

A Navier-type closed form solution is obtained via substitution of harmonic expressions for the displacements and temperature as well as considering materials with $C_{16} = C_{26} = C_{36} = C_{45} = 0$ and $\lambda_{pp3} = \lambda_{pn3} = 0$.

The following harmonic assumptions can be made for the field variables that

correspond to simply supported boundary conditions:

$$u_{\alpha_\tau}^k = \sum_{m,n}(\hat{U}_{\alpha_\tau}^k)\cos\left(\frac{m\pi\alpha_k}{a_{\alpha k}}\right)\sin\left(\frac{n\pi\beta_k}{b_{\beta k}}\right), \qquad k = 1, N_l,$$

$$u_{\beta_\tau}^k = \sum_{m,n}(\hat{U}_{\beta_\tau}^k)\sin\left(\frac{m\pi\alpha_k}{a_{\alpha k}}\right)\cos\left(\frac{n\pi\beta_k}{b_{\beta k}}\right), \qquad \tau = t, b, r,$$

$$u_{z_\tau}^k = \sum_{m,n}(\hat{U}_{z_\tau}^k)\sin\left(\frac{m\pi\alpha_k}{a_{\alpha k}}\right)\sin\left(\frac{n\pi\beta_k}{b_{\beta k}}\right), \qquad r = 2, N,$$

$$\theta_\tau^k = \sum_{m,n}(\hat{\theta}_\tau^k)\sin\left(\frac{m\pi\alpha_k}{a_{\alpha k}}\right)\sin\left(\frac{n\pi\beta_k}{b_{\beta k}}\right), \tag{43}$$

where $\hat{U}_{\alpha_\tau}^k$, $\hat{U}_{\beta_\tau}^k$, $\hat{U}_{z_\tau}^k$ and $\hat{\theta}_\tau^k$ are the amplitudes, m and n the wave numbers, and $a_{\alpha k}$ and $b_{\beta k}$ the shell dimensions.

The closed-form of fundamental nuclei $\boldsymbol{K}_{uu}^{k\tau s}(3 \times 3)$ and $\boldsymbol{K}_{u\theta}^{k\tau s}(3 \times 1)$ are given in Brischetto and Carrera [2009].

5. Results and discussion

For all the cases proposed in this section, the temperature amplitude imposed on the top surface is $+0.5$, and -0.5 on the bottom. In the case of assumed temperature profile (T_a), it is always considered linear from the top to the bottom as indicated in Fig. 3. In the case of calculated temperature profile (T_c), it is obtained by solving Fourier's heat conduction equation, as described in Section 3. The thus-calculated temperature profile is always approximated in Layer Wise form, even though the employed theory for the displacements is in Equivalent Single Layer form. The order of expansion used to approximate the temperature profile is the same as that of the displacements. The temperature profile in the plane (α, β) is always considered bi-sinusoidal with wave numbers $m = n = 1$.

Preliminary assessment

The employed theories in the proposed tables have already been validated for the thermo-mechanical analysis of composite shells in the companion paper by Brischetto and Carrera [2009]. The proposed refined kinematic models obtained by CUF have been compared to theories proposed by Khare *et al.* [2003] and Khdeir [1996] in the case of composite shells with an assumed linear profile of temperature through the thickness. The effectiveness of CUF to treat such problems is clearly reported in Brischetto and Carrera [2009]. These validated models can be used with confidence to study the effects of the through-the-thickness temperature distribution on the response of composite shells.

Case 1: isotropic one-layered cylindrical shell

The considered shell has dimensions $a_\alpha = 1$ and $b_\beta = \frac{\pi}{3}R_\beta = 10.47197551$. The radii of curvature in the α and β directions are $\frac{1}{R_\alpha} = 0$ and $\frac{1}{R_\beta} = 0.1$, respectively. The considered thicknesses are $h = 2.5, 1.0, 0.1, 0.01$, which means thickness ratios $R_\beta/h = 4, 10, 100, 1000$. The considered material is Aluminum $Al5086$ with Young's modulus $E = 70.3GPa$, Poisson's ratio $\nu = 0.33$, thermal expansion coefficient $\alpha = 24 \times 10^{-6}K^{-1}$ and conductivity coefficient $K = 130W/mK$. The transverse displacement $\bar{w}$ and the in-plane stress $\sigma_{\alpha\beta}$ are calculated in the middle of the shell in Table 1. Different thickness ratios R_β/h are investigated. Only ESL

Table 1. Case 1. Isotropic one-layered shell. Non-dimensional transverse displacement $\bar{w} = \frac{10u_z h}{a_\alpha^2 \alpha T_1}$ and in-plane stress $\sigma_{\alpha\beta}$ in $z = 0$. $T_1 = 1.0$ is the gradient of the linear temperature profile. Assumed linear temperature (T_a) vs calculated temperature profile (T_c) for different applied theories.

R_β/h		$\bar{w}$ 10	100	1000	$\sigma_{\alpha\beta}$ 10	100	1000
$ED4$	T_a	0.9468	1.2007	0.1151	$0.3209 * 10^4$	$0.1916 * 10^5$	$0.1822 * 10^5$
	T_c	0.9062	1.1987	0.1151	$0.2847 * 10^4$	$0.1913 * 10^5$	$0.1822 * 10^5$
$ED3$	T_a	0.9602	1.2007	0.1151	$0.3270 * 10^4$	$0.1916 * 10^5$	$0.1822 * 10^5$
	T_c	0.9415	1.9999	0.1151	$0.1379 * 10^5$	$0.1928 * 10^5$	$0.1822 * 10^5$
$ED2$	T_a	0.8398	1.1994	0.1151	$0.2976 * 10^4$	$0.1914 * 10^5$	$0.1822 * 10^5$
	T_c	0.8398	1.1994	0.1151	$0.2972 * 10^4$	$0.1914 * 10^5$	$0.1822 * 10^5$
$ED1$	T_a	1.9784	1.8359	0.2189	$0.4977 * 10^4$	$0.2244 * 10^5$	$0.2642 * 10^5$
	T_c	1.9784	1.8359	0.2189	$0.4977 * 10^4$	$0.2244 * 10^5$	$0.2642 * 10^5$
$FSDT$	T_a	1.9818	1.7943	0.1715	$0.4086 * 10^4$	$0.2846 * 10^5$	$0.2712 * 10^5$
	T_c	1.9818	1.7943	0.1715	$0.4086 * 10^4$	$0.2846 * 10^5$	$0.2712 * 10^5$
CLT	T_a	1.9869	1.7985	0.1716	$0.4087 * 10^4$	$0.2852 * 10^5$	$0.2713 * 10^5$
	T_c	1.9869	1.7985	0.1716	$0.4087 * 10^4$	$0.2852 * 10^5$	$0.2713 * 10^5$

theories are reported in the table because the shell is one-layered. T_a means a linear assumed temperature profile in the thickness direction, T_c means a calculated temperature approximated in the thickness direction with the same order as the employed kinematic model. In the case of a one-layered shell, when the structure is very thin, the assumed profile T_a coincides with the calculated T_c one, therefore a thin shell means a linear temperature profile through the thickness. For thick shells, the difference between profiles T_a and T_c is much more evident, as illustrated in Fig. 4 which clearly explains the results of Table 1; there are two sources of error for the thermo-mechanical analysis of one-layered homogeneous shells: - the employed kinematic model for the displacement; - the considered temperature profile. For thick shells, the temperature profile is not linear and it must be calculated by Fourier's equation and then approximated with a higher order of expansion (N=4). The transverse displacement $\bar{w}$ through the thickness z is reported in Fig. 5 for the case of a thick and thin shell, respectively. Fig. 5 clearly shows two main aspects for the thermo-mechanical analysis of shells: - assumed vs calculated temperature profile; - the importance of a higher-order of expansion for the unknowns.
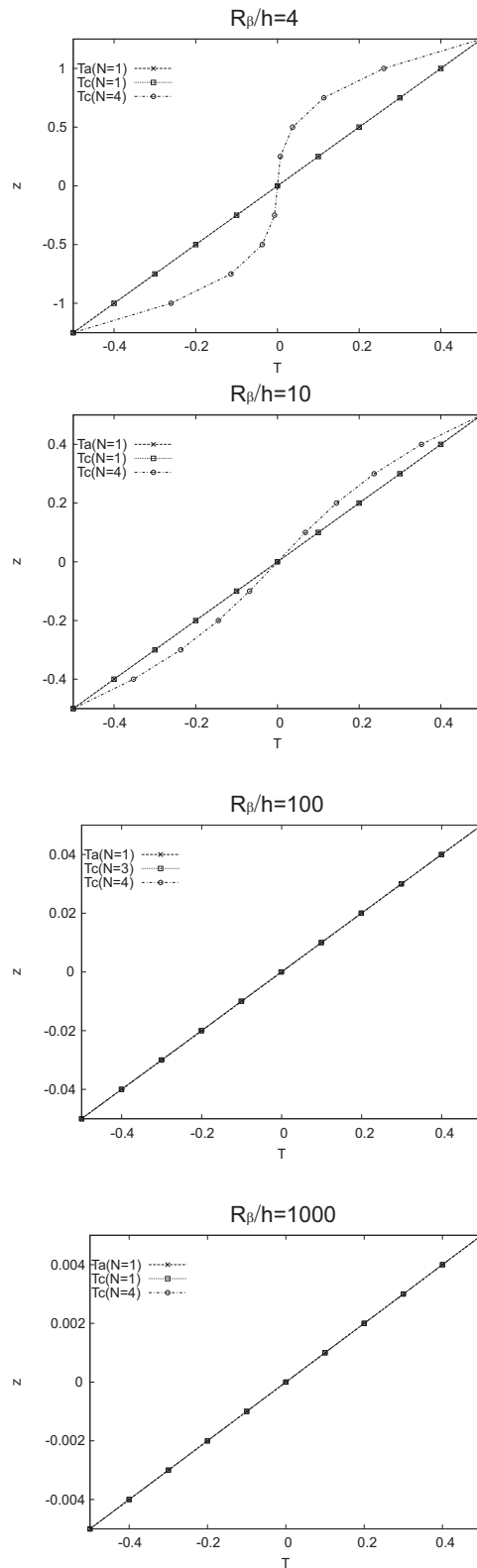
Fig. 4.   Case 1. Assumed linear temperature (T_a) vs calculated temperature profile (T_c) for one-layered isotropic cylindrical shell in case of $R_\beta/h = 4, 10, 100, 1000$. N is the order of expansion employed to approximate the temperature profile.
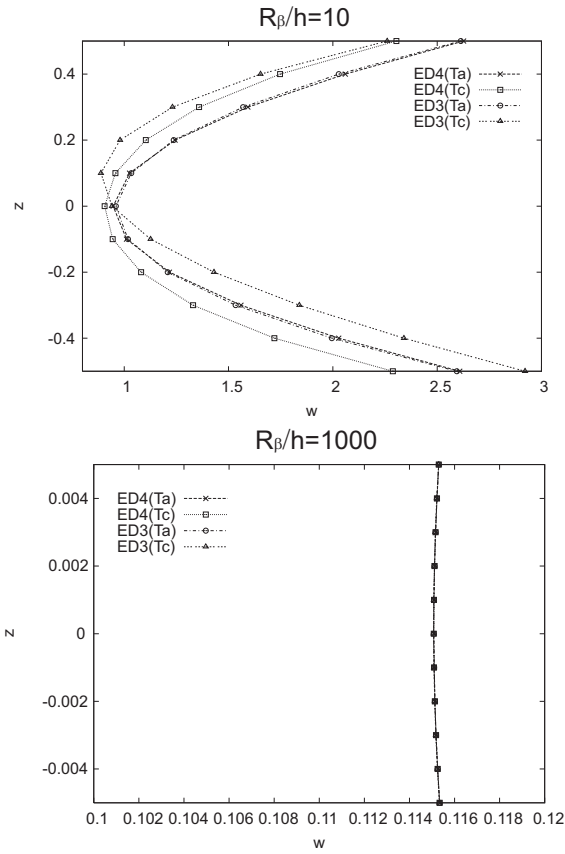
Fig. 5. Case 1. Isotropic one-layered cylindrical shell. Non-dimensional transverse displacement $\bar{w}$ through z for $R_\beta/h = 10$ and $R_\beta/h = 1000$. Assumed temperature profile (T_a) vs calculated temperature profile (T_c) for refined models.

Case 2: isotropic two-layered cylindrical shell

The considered shell has the same dimensions and geometrical properties as the shell indicated in case 1. The considered total thicknesses are $h = 2.5, 1.0, 0.1, 0.01$ which means thickness ratios $R_\beta/h = 4, 10, 100, 1000$. The bottom layer is in $Al5086$ (the same as case 1) while the top layer is in Titanium $Ti22$ with Young's modulus $E = 110.GPa$, Poisson's ratio $\nu = 0.32$, thermal expansion coefficient $\alpha = 8.6 \times 10^{-6}K^{-1}$ and conductivity coefficient $K = 21.9W/mK$. The two considered layers have the same thickness $h/2$. The non-dimensioned quantities in the tables and figures are dimensioned with the data of aluminum $Al5086$. Non-dimensioned transverse displacement $\bar{w}$ is considered in $z = h/4$ in Table 2. In this analysis, both LW and ESL models are considered because the shell is two-layered. The difference between LW and ESL models, and between the assumed and calcu-

Table 2.   Case 2. Two-layered isotropic shell in aluminium and titanium. Non-dimensional transverse displacement $\bar{w} = \frac{10 u_z h}{a_\alpha^2 \alpha_{Al} T_1}$ in $z = h/4$. Equivalent Single Layer vs Layer Wise Theories. $T_1 = 1.0$ is the gradient of the linear temperature profile. Assumed linear temperature (T_a) vs calculated temperature profile (T_c) for different applied theories.

R_β/h		4	10	100	1000
			ESL theories		
$ED4$	T_a	0.4068	0.7416	0.7468	0.0325
	T_c	0.3075	0.6127	0.7947	-0.0533
$ED3$	T_a	0.4170	0.7428	0.7470	0.0325
	T_c	0.2273	0.5960	0.7941	-0.0535
$ED2$	T_a	-0.3183	0.5089	0.7465	0.0326
	T_c	-0.2408	0.4300	0.7930	-0.0535
$ED1$	T_a	1.0680	1.1867	1.1525	0.0956
	T_c	1.0504	1.1871	1.3021	0.0254
$FSDT$	T_a	1.2351	1.2694	1.1054	0.0463
	T_c	1.2418	1.3566	1.1884	-0.0797
CLT	T_a	1.2908	1.2914	1.1096	0.0463
	T_c	1.3017	1.3956	1.1966	-0.0797
			LW Theories		
$LD4$	T_a	0.4002	0.7472	0.7468	0.0325
	T_c	0.3977	0.6385	0.7952	-0.0530
$LD3$	T_a	0.4242	0.7487	0.7468	0.0325
	T_c	0.2982	0.6354	0.7951	-0.0530
$LD2$	T_a	0.3999	0.7351	0.7467	0.0325
	T_c	0.3201	0.5780	0.7938	-0.0530
$LD1$	T_a	0.3514	0.7319	0.8630	0.0487
	T_c	0.3407	0.7053	0.8724	-0.0400

lated temperature profile are clearly shown in Table 2. In this case, even though a thin shell is considered, there is a difference between the results obtained with T_a and those obtained with T_c. This fact is clearly explained in Fig. 6: the calculated temperature profile for thin shells is linear in each layer, but its slope changes because the layer in $Al5086$ has a different conductivity coefficient K from the K of the layer in $Ti22$. A different K means different slopes because of the continuity of flux q_z in Eq.(11), in this case the two layers have two different values of the transverse conductivity coefficient K. Eqs.(19) and (23) clearly explain why the temperature profile is linear for each layer when the shell is thin but with different slopes. The in-plane stress $\sigma_{\alpha\beta}$, through the thickness z, is reported in Fig. 7 for both thick and thin shells. Because of what is explained in Fig. 6, the differences between an assumed and a calculated temperature profile, even though the shell is thin, are confirmed.
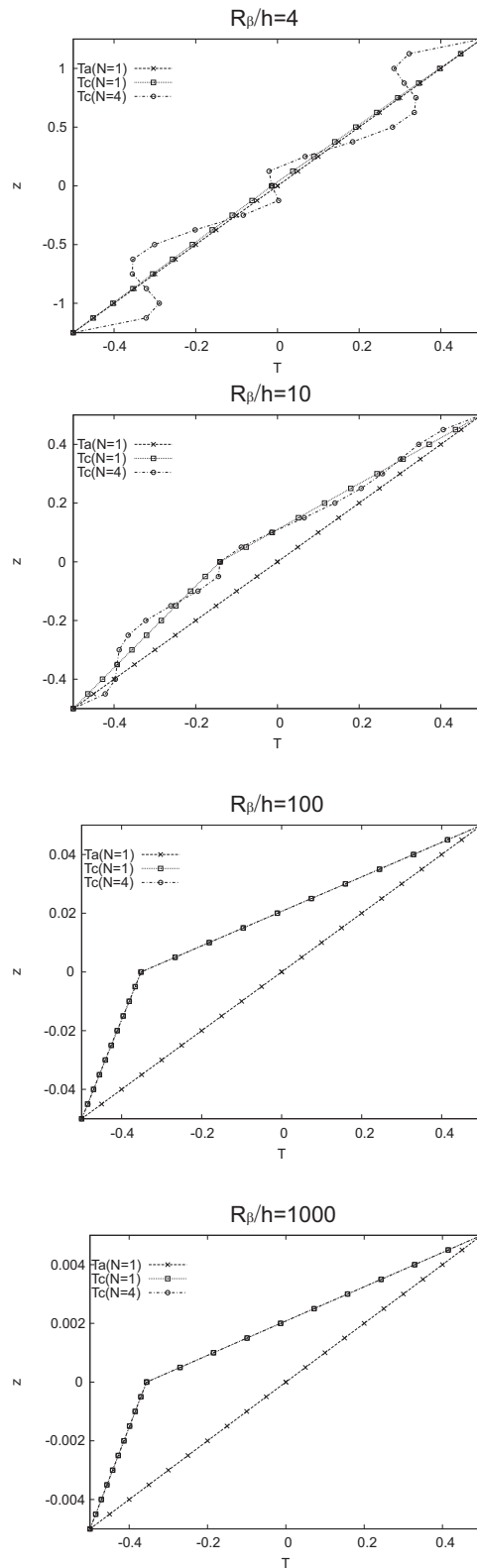
Fig. 6.   Case 2. Assumed linear temperature (T_a) vs calculated temperature profile (T_c) for two-layered isotropic cylindrical shell in case of $R_\beta/h = 4, 10, 100, 1000$. N is the order of expansion employed to approximate the temperature profile.
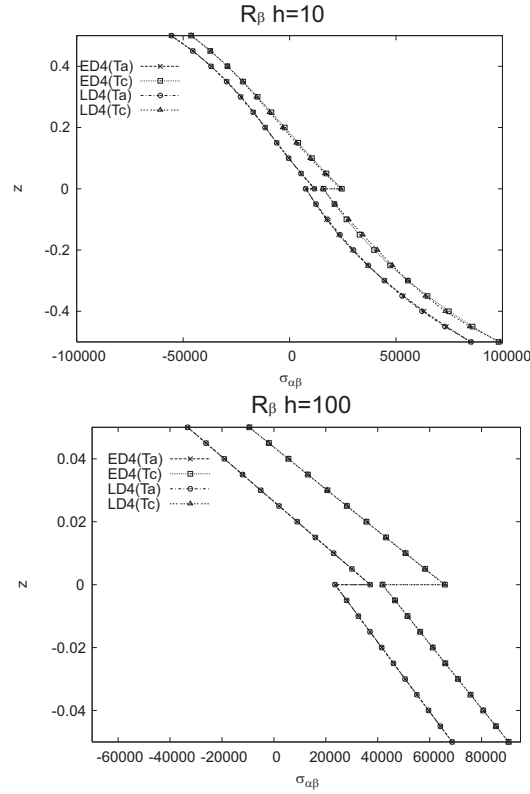
Fig. 7.   Case 2. Isotropic two-layered cylindrical shell. In-plane stress $\sigma_{\alpha\beta}$ through z for $R_\beta/h = 10$ and $R_\beta/h = 100$. Assumed temperature profile (T_a) vs calculated temperature profile (T_c) for refined models.

Case 3: cylindrical shell with two carbon fiber reinforced layers (0°/90°)

The proposed shell has dimensions $a_\alpha = b_\beta = 1$. The radii of curvature in the α and β directions are $\frac{1}{R_\alpha} = 0$ and $\frac{1}{R_\beta} = 0.2, 0.1, 0.02$. The considered total thicknesses is $h = 0.1$. The ratio between Young's modulus in the longitudinal and transverse direction is $E_L/E_T = 25.0$. The shear modulus ratio is $G_{LT}/G_{TT} = 2.5$, Poisson's ratio is $\nu_{LT} = \nu_{TT} = 0.25$. The ratio between the thermal expansion coefficient in the transverse and longitudinal direction is $\alpha_T/\alpha_L = 3.0$. The conductivity coefficients are $K_L = 36.42W/mK$ in the longitudinal direction and $K_T = 0.96W/mK$ in the transverse direction. The two layers have the same thickness $h/2$ with sequence lamination 0°/90°. If we consider Fig. 8, it is clearly indicated that the assumed and calculated temperature profiles are close for a thin shell, but not coincident. The two layers are made of the same material and when the fiber orientation changes from 0° to 90°, the value of the transverse conductivity coefficient K_3 does not change
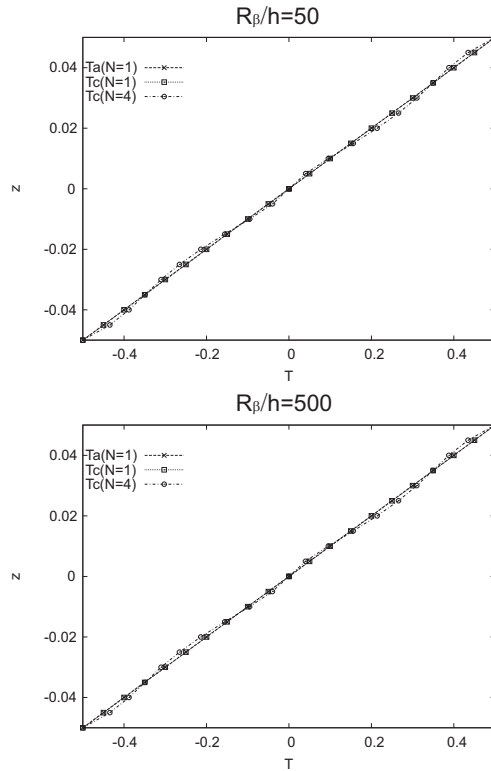
Fig. 8.   Case 3. Assumed linear temperature (T_a) vs calculated temperature profile (T_c) for two-layered composite fiber reinforced cylindrical shell in case of $R_\beta/h = 50, 500$. N is the order of expansion employed to approximate the temperature profile.

and it is the same in the continuity of the transverse heat flux in Eq.(23). Moreover, if we consider Eq.(19), the coefficient s_1^k does not change because $m = n = 1$ and $a = b = 1$, therefore when the fiber orientation changes from $0°$ to $90°$, the coefficients K_1 and K_2 multiply the same quantities. These aspects explain Table 3: the LD1 and ED1 theories with T_a and T_c give the same results for thin and moderately thick shells. The slope of the temperature profile does not change in fact from one layer to another. Due to the two layers, the temperature profile is never linear (even though the shell is thin) and this means that the same theory gives different results, depending on the choice of the T_a or T_c profile. The solution added in the Table 3, called HOST12, is an ESL model with cubic expansion in z direction for the three displacement components (similar to the ED3 model obtained by CUF). In Khare *et al.* [2003] for the HOST12 only an assumed temperature profile has been employed, and this limitation is clearly outlined in Table 3. The difference for the transverse displacement $\bar{w}$ through the thickness z, in the case of a linear temperature profile

Table 3. Case 3. Two-layered carbon fiber reinforced cylindrical shell $(0°/90°)$. Non-dimensional transverse displacement $\bar{w} = \frac{u_z}{b_\beta^2 \alpha_L T_1}$ in $z = 0$. Equivalent Single Layer vs Layer Wise theories. $T_1 = 1.0$ is the gradient of the linear temperature profile. Assumed linear temperature (T_a) vs calculated temperature profile (T_c) for different applied theories.

R_β/h		50	100	500
		ESL theories		
$HOST12$[Khare *et al.*, 2003]	T_a	1.1261	1.1434	1.1493
	T_c	−	−	−
$ED4$	T_a	1.1276	1.1434	1.1479
	T_c	1.1173	1.1328	1.1371
$ED3$	T_a	1.1264	1.1422	1.1466
	T_c	1.1255	1.1416	1.1463
$ED2$	T_a	1.1255	1.1411	1.1455
	T_c	1.0894	1.1042	1.1083
$ED1$	T_a	1.1806	1.1959	1.1997
	T_c	1.1807	1.1959	1.1997
$FSDT$	T_a	1.1805	1.1959	1.1997
	T_c	1.1806	1.1959	1.1997
CLT	T_a	1.1834	1.1966	1.1997
	T_c	1.1834	1.1966	1.1997
		LW theories		
$LD4$	T_a	1.1280	1.1434	1.1477
	T_c	1.1179	1.1331	1.1373
$LD3$	T_a	1.1280	1.1434	1.1477
	T_c	1.1271	1.1428	1.1474
$LD2$	T_a	1.1262	1.1414	1.1457
	T_c	1.0911	1.1056	1.1095
$LD1$	T_a	1.1425	1.1577	1.1620
	T_c	1.1425	1.1578	1.1620

and a calculated profile with $N = 4$ approximation in the thickness direction, is shown in Fig. 9.

Case 4: cylindrical shell with ten carbon fiber reinforced layers $(0°/90°)$

The geometry and material properties of this cylindrical shell are the same as case 3. In this case, ten carbon fiber reinforced layers are considered with sequence lamination $0°/90°$, the total thickness h is the same as case 3 and each layer has a thickness $h/10$. The results of the transverse displacement $\bar{w}$ are reported in Table 4. The assumed and calculated temperature profile are never the same because of the 10 layers. The difference between the T_a and T_c profiles is clearly reported in Fig. 10 which clearly explains Table 4: the importance of LW theories, a high order of expansions and a calculated temperature profile T_c for the analysis of multilayered composite shells. As for the case 3, the HOST12 model [Khare *et al.*, 2003] has been added to demonstrate the inadequacy of an assumed temperature profile T_a

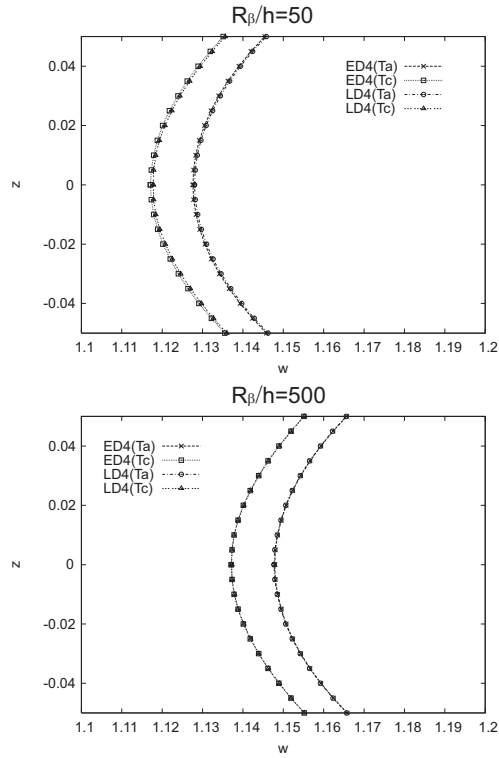24 *Salvatore Brischetto*

Fig. 9.   Case 3. Two-layered carbon fiber reinforced cylindrical shell. Non-dimensional transverse displacement $\bar{w}$ through z for $R_\beta/h = 50$ and $R_\beta/h = 500$. Assumed temperature profile (T_a) vs calculated temperature profile (T_c) for refined models.

for such problems. The in-plane stress $\sigma_{\alpha\beta}$ through z is given in Fig. 11 for thin and very thin shells. The same conclusions obtained for displacements are confirmed for case of stresses.

6. Conclusions

The effects of a through-the-thickness temperature in multilayered shells have been analyzed in this paper. Having imposed the values of temperature at the top and bottom surfaces of the shell, two different profiles have been compared: - an assumed linear profile from the top to the bottom that does not depend on the number of layers; - a layer-wise profile, with orders of expansion from linear to fourth, which approximate the temperature profile in the thickness direction calculated by Fourier's heat conduction equation. The importance of refined models for the thermal bending of multilayered shells has been confirmed. The importance of calculating the actual temperature profile to obtain a correct thermal loading has been shown by

Table 4.   Case 4. Ten-layered carbon fiber reinforced cylindrical shell (lamination sequence: $0°/90°$). Non-dimensional transverse displacement $\bar{w} = \frac{u_z}{b_\beta^2 \alpha_L T_1}$ in $z = 0$. Equivalent Single Layer vs Layer Wise theories. $T_1 = 1.0$ is the gradient of the linear temperature profile. Assumed linear temperature (T_a) vs calculated temperature profile (T_c) for different applied theories.

R_β/h		50	100	500
		ESL theories		
$HOST12$[Khare *et al.*, 2003]	T_a	1.0224	1.0299	1.0325
	T_c	−	−	−
$ED4$	T_a	1.0208	1.0279	1.0301
	T_c	0.9642	0.9709	0.9730
$ED3$	T_a	1.0208	1.0279	1.0301
	T_c	0.9640	0.9707	0.9728
$ED2$	T_a	1.0184	1.0251	1.0271
	T_c	0.9572	0.9634	0.9654
$ED1$	T_a	1.0468	1.0533	1.0551
	T_c	0.9872	0.9933	0.9951
$FSDT$	T_a	1.0468	1.0533	1.0551
	T_c	0.9872	0.9933	0.9951
CLT	T_a	1.0496	1.0540	1.0552
	T_c	0.9898	0.9940	0.9951
		LW theories		
$LD4$	T_a	1.0207	1.0283	1.0306
	T_c	0.9643	0.9715	0.9737
$LD3$	T_a	1.0207	1.0283	1.0306
	T_c	0.9643	0.9715	0.9737
$LD2$	T_a	1.0207	1.0283	1.0306
	T_c	0.9613	0.9684	0.9706
$LD1$	T_a	1.0207	1.0283	1.0306
	T_c	0.9644	0.9715	0.9737

comparing various shell configurations.

Reference

Barut, A., Madenci, E. and Tessler, A. [2000] "Nonlinear thermoelastic analysis of composite panels under non-uniform temperature distribution," *International Journal of Solids and Structures*, **37**(27), 3681–3713.

Birsan, M. [2009] "Thermal stresses in cylindrical Cosserat elastic shells," *European Journal of Mechanics A/Solids*, **28**(1), 94–101.

Brischetto, S., Leetsch, R., Carrera, E., Wallmersperger, T. and Kröplin, B. [2008] "Thermo-mechanical bending of functionally graded plates," *Journal of Thermal Stresses*, **31**(3), 286–308.

Brischetto, S. and Carrera, E. [2009] "Thermal stress analysis by refined multilayered composite shell theories," *Journal of Thermal Stresses*, **32**(1-2), 165–186.

Carrera, E. [1995] "A class of two dimensional theories for multilayered plates anal-

26   *Salvatore Brischetto*

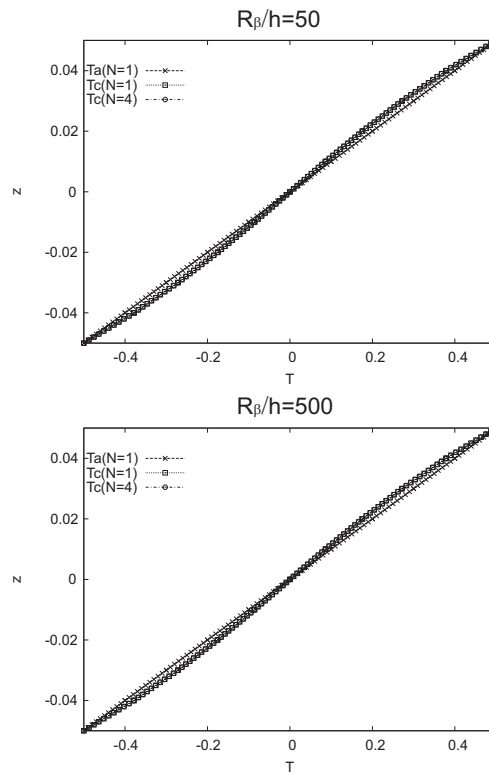

Fig. 10.   Case 4. Assumed linear temperature (T_a) vs calculated temperature profile (T_c) for ten-layered composite fiber reinforced cylindrical shell in case of $R_\beta/h = 50, 500$. N is the order of expansion employed to approximate the temperature profile.

ysis," *Atti Accademia delle Scienze di Torino, Memorie Scienze Fisiche*, **19-20**, 49–87.

Carrera, E. [2000] "An assessment of mixed and classical theories for the thermal stress analysis of orthotropic multilayered plates," *Journal of Thermal Stresses*, **23**(9), 797–831.

Carrera, E. [2002a] "Theories and finite elements for multilayered anisotropic, composite plates and shells," *Archives of Computational Methods in Engineering*, **9**(2), 87–140.

Carrera, E. [2002b] "Temperature profile influence on layered plates response considering classical and advanced theories," *AIAA Journal*, **40**(9), 1885–1856.

Carrera, E. and Brischetto, S. [2008a] "Analysis of thickness locking in classical, refined and mixed multilayered plate theories," *Composite Structures*, **82**(4), 549–562.

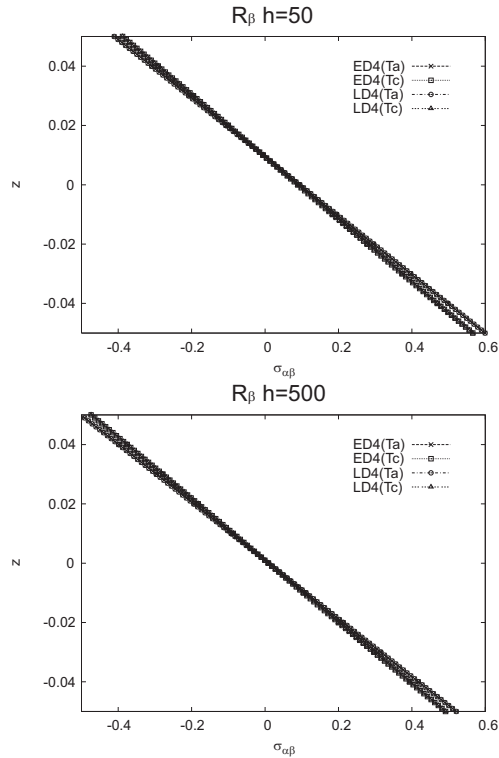Carrera, E. and Brischetto, S. [2008b] "Analysis of thickness locking in classical,

Fig. 11.   Case 4. Ten-layered carbon fiber reinforced cylindrical shell. In-plane stress $\sigma_{\alpha\beta}$ through z for $R_\beta/h = 50$ and $R_\beta/h = 500$. Assumed temperature profile (T_a) vs calculated temperature profile (T_c) for refined models.

refined and mixed theories for layered shells," *Composite Structures*, **85**(1), 83–90.

Cheng, Z. Q. and Batra, R. C. [2001] "Thermal effects on laminated composite shells containing interfacial imperfections," *Composite Structures*, **52**(1), 3–11.

Ding, K. [2008] "Thermal stresses of weak formulation study for thick open laminated shell," *Journal of Thermal Stresses*, **31**(4), 389–400.

Dumir, P. C., Nath, J. K., Kumari, P. and Kapuria, S. [2008] "Improved efficient zigzag and third order theories for circular cylindrical shells under thermal loading," *Journal of Thermal Stresses*, **31**(4), 343–367.

Holstein, D., Aswendt, P., Hofling, R., Schmidt, C. D. and Jiiptner, W. [1998] "Deformation analysis of thermally loaded composite tubes," *Composite Structures*, **40**(3), 257–265.

Hsu, Y. S., Reddy, J. N. and Bert, C. W. [1981] "Thermoelasticity of circular cylindrical shells laminated of bimodulus composite materials," *Journal of Thermal*

Stresses, **4**(2), 155–177.

Iesan, D. [1985] "Thermal stresses in heterogeneous anisotropic Cosserat elastic cylinders," *Journal of Thermal Stresses*, **8**(4), 385–397.

Kapuria, S., Sengupta, S. and Dumir, P. C. [1997] "Three-dimensional solution for a hybrid cylindrical shell under axisymmetric thermoelectric load," *Archive of Applied Mechanics*, **67**(5), 320–330.

Khare, R. K., Kant, T. and Garg, A. K. [2003] "Closed-form thermo-mechanical solutions of higher-order theories of cross-ply laminated shallow shells," *Composite Structures*, **59**(3), 313–340.

Khdeir, A. A., Rajab, M. D. and Reddy, J. N. [1992] "Thermal effects on the response of cross-ply laminated shallow shells," *International Journal of Solids and Structures*, **29**(5), 653–667.

Khdeir, A. A. [1996] "Thermoelastic analysis of cross-ply laminated circular cylindrical shells," *International Journal of Solids and Structures*, **33**(27), 4007–4017.

Leissa, A. W. [1973] *Vibration of shells*, (NASA SP-288, National Aeronautics and Space Administration, Washington (USA)).

Librescu, L. and Lin, W. [1999] "Non-linear response of laminated plates and shells to thermomechanical loading: implications of violation of interlaminar shear traction continuity requirement," *International Journal of Solids and Structures*, **36**(27), 4111–4147.

Librescu, L. and Marzocca, P. [2003a] *Thermal stresses'03*, (vol.1, Virginia Polytechnic Institute and State University, Blacksburg, VA (USA)).

Librescu, L. and Marzocca, P. [2003b] *Thermal stresses'03*, (vol.2, Virginia Polytechnic Institute and State University, Blacksburg, VA (USA)).

Miller, C. J., Millavec, W. A. and Richer, T. P. [1981] "Thermal stress analysis of layered cylindrical shells," *AIAA Journal*, **19**(4), 523–530.

Noor, A. K. and Burton, W. S. [1992] "Computational models for high-temperature multilayered composite plates and shells," *Applied Mechanics Reviews*, **45**(10), 419–446.

Padovan, J. [1976] "Thermoelasticity of cylindrically anisotropic generally laminated cylinders," *Journal of Applied Mechanics*, **43**, 124–130.

Pelletier, J. L. and Vel, S. S. [2006] "An exact solution for the steady-state thermoelastic response of functionally graded orthotropic cylindrical shells," *International Journal of Solids and Structures*, **43**(5), 1131–1158.

Reddy, J. N. [2004] *Mechanics of laminated composite plates and shells*, (CRC Press, New York (USA)).

Rolfes, R., Noack, J. and Taeschner, M. [1999] "High performance 3D-analysis of thermo-mechanically loaded composite structures," *Composite Structures*, **46**(4), 367–379.

Rolfes, R. and Rohwer, K. [2000] "Integrated thermal and mechanical analysis of

composite plates and shells," *Composites Science and Technology*, **60**(11), 2097–2106.

Santos, H., Mota Soares, C. M., Mota Soares, C. A. and Reddy, J. N. [2008] "A semi-analytical finite element model for the analysis of cylindrical shells made of functionally graded materials under thermal shock," *Composite Structures*, **86**(1-3), 10–21.

Shen, H. S. [2005] "Postbuckling of axially loaded FGM hybrid cylindrical shells in thermal environments," *Composites Science and Technology*, **65**(11-12), 1675–1690.

Shen, H. S. and Noda, N. [2005] "Postbuckling of FGM cylindrical shells under combined axial and radial mechanical loads in thermal environments," *International Journal of Solids and Structures*, **42**(16-17), 4641–4662.

Shen, H. S. and Noda, N. [2007] "Postbuckling of pressure-loaded FGM hybrid cylindrical shells in thermal environments," *Composite Structures*, **77**(4), 546–560.

Vel, S. S. and Pelletier, J. L. [2007] "Multi-objective optimization of functionally graded thick shells for thermal loading," *Composite Structures*, **81**(3), 386–400.

Wu, L., Jiang, Z. and Liu, J. [2005] "Thermoelastic stability of functionally graded cylindrical shells," *Composite Structures*, **70**(1), 60–68.

Zhen, W. and Wanji, C. [2008] "A global-local higher order theory for multilayered shells and the analysis of laminated cylindrical shell panels," *Composite Structures*, **84**(4), 350–361.